RESEARCH ON CENTERLINE EXTRACTION OF MAIZE SEEDLING ROW AT 3-5 LEAF STAGE BASED ON IMPROVED RANSAC

Ruitao MA[1], Aoran GUO[2],Bing ZHAO[3], Yanfei ZHANG[4], Jinliang GONG[5*]

To address the issues of insufficient real-time performance and inaccurate machine vision when extracting navigation lines for 3-5 leaf maize seedlings in complex environments, this study introduces a centerline extraction algorithm for maize seedlings that is based on an enhanced RANSAC method. Initially, enhancements are applied to the conventional 2G-R-B algorithm, followed by the implementation of morphological processing and the maximum inter-class variance method for image noise reduction. To address the issue of low reliability in the conventional method of obtaining the region of interest, we propose establishing a color threshold range in the HSV space transformation. Additionally, we suggest employing the mask operation to extract the green features. This will compensate for the information lost by the hyper-greening algorithm, which is influenced by interference. Furthermore, we can determine the dynamic region of interest by applying a pixel threshold constraint. The RANSAC algorithm has been enhanced, and the iterative optimization is continuously refined to extract the internal points and eliminate the external points in order to more accurately determine the clustering center of the corn seedling belt. The robust regression method is employed to fit the navigation line of the cluster center. Experiments demonstrate that the algorithm possesses a robust anti-interference capability and is capable of adapting to the intricate and fluctuating environment. Furthermore, its accuracy can reach as high as 95.12%. The processing time for an image with a resolution of 640 pixels × 480 pixels is merely 83.61ms. The algorithm presented in this paper offers a trustworthy and real-time navigation path for the robot to navigate through the cornfield.

Keywords: machine vision, morphological processing, navigation, the RANSAC algorithm, the robust regression method

[1]School of Mechanical Engineering, Shandong University of Technology, Zibo 255049, China, e-mail: 13345107835@163.com
[2]School of Agricultural Engineering and Food Science, Shandong University of Technology, Zibo 255049, China, e-mail: gar1051695085@163.com
[3]School of Mechanical Engineering, Shandong University of Technology, Zibo 255049, China, e-mail: 18353732642@163.com
[4]School of Agricultural Engineering and Food Science, Shandong University of Technology, Zibo 255049, China, e-mail: 1392076@sina.com
[5*]Prof., School of Mechanical Engineering, Shandong University of Technology, Zibo 255049, China, e-mail: 84374294@qq.com (corresponding author)

1.Introduction

Agricultural machinery with automatic navigation technology is widely used in tasks such as weeding, sowing, harvesting, and other activities on farmland [1]. Agriculture is considered one of the most fundamental and vital industries in human society. As a crucial component of modern technology, autonomous navigation in agriculture is slowly transforming the methods and effectiveness of agricultural production. Domestic and international scholars have extensively researched visual navigation technology [2-4]. In comparison to GPS and LIDAR, visual navigation technology offers the advantages of easy operation and affordability. Meeting the demands of modern agriculture's development, the autonomous movement of weeding machines has emerged as the primary focus of intelligent agricultural mechanization research. Automatic navigation plays a vital role in the autonomous driving of a weeding machine. Science and technology serve as the primary driving forces to enhance agricultural development, and agricultural mechanization is an effective approach to achieving scientific and technological progress. Therefore, the smartification of agricultural machinery plays an irreplaceable role in advancing modern agricultural science and technology [5]. Automatic navigation of agricultural machinery is the foundation and essential technology for achieving autonomous control and intelligent operation of agricultural machinery in farming environments. It holds immense importance in driving the development of ‘precision agriculture’. With the rapid development of vision and other sensor technologies, automatic navigation technology for agricultural machinery is becoming increasingly mature. The realization of automatic navigation in agricultural machinery is helpful to reduce reliance on labor and weather conditions, greatly improve operational efficiency, and play a significant role in promoting the development of precision agriculture [6].

Given that maize is typically planted in straight rows in China, it can play a critical role in aiding automated navigation by helping identify the central row of maize crop lines and obtaining crucial location data [7]. Scholars from both domestic and international institutions have conducted extensive research on the extraction of row crop centerlines. The most frequently employed approach is the crop row centerline detection method utilizing the Hough transform technique. This particular method is widely used in the field of image processing. The Hough transform is able to map the pixels to the parameter space, which includes the slope and intercept of a straight line. By conducting a statistical analysis on the parameter space and applying an appropriate threshold, it is possible to determine the best fitting straight line, specifically the center line of the crop row [8-10]. However, the standard Hough algorithm has limitations in terms of calculation accuracy, complexity, and real-time performance. Moreover, the complex terrain environment

found in farmland poses challenges when it comes to accurately extracting the center line of crop rows.

Lai Hanrong et al [11] utilized a method for real-time identification and navigation of corn seedling belts. This method was based on updating the region of interest. The seedling belt image was enhanced to have a vibrant green color and was standardized. The traditional SUSAN corner point method was enhanced to eliminate unnecessary outlier feature points. Then, the feature points were grouped together in a sequential manner to determine the navigation line. The region of interest was updated in real-time using clustering analysis. The accuracy of this navigation line extraction was exceptionally high, reaching 96.8%. Gong Jinliang et al [12] utilized corner detection and gradient descent to extract the navigation line. They then employed the random sampling consistent algorithm to fit the navigation line. This method demonstrates real-time capability and robustness, with an accuracy rate as high as 92.2%. Liu Yiting et al [13] utilized a combination of various algorithms, including balanced pixel grayscale histogram, super green eigen factor, genetic annealing, etc., in order to successfully extract navigation lines in corn rows.

The aforementioned methods have yielded certain results in extracting navigation lines, but there exist limitations when dealing with complex environments like farmland, thereby making it challenging to achieve satisfactory outcomes [14]. To enhance the precision and accuracy of acquiring navigation lines, this paper suggests a navigation line extraction method centered around the RANSAC algorithm. This algorithm is known for its high accuracy, real-time functionality, decreased susceptibility to interference points, and ability to closely fit the navigation line.

2. Image preprocessing

2.1 Graying of farmland images

In the visual navigation system of weeding robots, grayscale images are commonly utilized for depth processing to enhance efficiency and accuracy in processing. The contrast and clarity of the image can be enhanced by grayscale transformation, which effectively emphasizes and analyzes the morphology and texture of objects. This, in turn, facilitates the extraction of navigation lines on the road. This approach eliminates the computational and storage load associated with color images and simplifies the complexity of image processing. In a corn field, a corn seedling appears green, as natural colors are typically made up of the primary colors red, green, and blue. Assuming that the color of a pixel point is represented as RGB(r,g,b), we obtain a gray value by calculating the three color channels of the point according to a specific rule. In this process, the values for r, g, and b in the original RGB(r,g,b) are uniformly replaced with gray, resulting in a new color

RGB(gray, gray, gray). This process allows us to determine the grayscale value of the color at the given point[15]. In the RGB color space, the G component of the original image of the corn seedling is larger than the R and B components. According to this feature, the proportion of the G component is appropriately increased during the image gray scaling process to better distinguish the corn seedling from the soil background [16]. This paper presents an improved version of the Excess green grayscale algorithm (EXG). The purpose of this enhancement is to emphasize the crop features while minimizing the impact of the background color (as demonstrated in Equation (1)). Drawing from the original method, we enhanced the G component and suppressed the R component to improve the differentiation between green plants and soil, taking into account the relatively prominent R component of soil. Additionally, we employed a method to calculate the grayscale value in order to minimize the grayscale variance among different parts of the same plant. The formula is as follows:

$$gray(x,y)=\begin{cases}2G(x,y)-R(x,y)-B(x,y) & else\\ 255 & 2G-R-B>255\\ 0 & 2G-R-B<0\end{cases} \tag{1}$$

and

$$gray(x,y)=\begin{cases}2G(x,y)-B(x,y) & G>R\ or\ G>B\\ 0 & else\end{cases} \tag{2}$$

In the formula, gray (x, y) represents the brightness value of the grayscale image. R (x, y) corresponds to the red component in the RGB color space, B (x, y) denotes the blue component, and G (x, y) signifies the green component.
Subsequently, we applied the enhanced 2G-R-B algorithm to process the image of the green corn seedling belt and compared the resulting images. The comparison results are illustrated in Fig.1:

a. Original images b. Gray-scale image

Fig.1 Comparison of farmland image gray processing

Observing Fig.1, we can infer that while the 2G-R-B algorithm successfully isolates the green plants from the soil backgrounds, it falls short in accurately delineating the contours of the corn seedlings. Particularly, the algorithm struggles to capture the intricate details of the green leaves, failing to fully convey the original image information.

2.2 Image binarization and noise filtering

Binarization image is an important step in digital image processing. Commonly used binarization algorithms encompass the global fixed threshold method, adaptive threshold method, bimodal method, Otsu's method, and others. In this paper, the improved maximum inter-class variance method (Ostu) is used to segment the corn seedling belt and soil, and the binary image is obtained. The unstructured nature of farmland entails the presence of various interference factors, such as wheat straw and weeds growing amidst corn rows. Additionally, corn seedlings may exhibit noise in the form of small holes. To effectively remove the aforementioned holes and noise, this research paper employs morphological expansion and erosion operations. The formula for these operations is as follows:

$$A\square \mathrm{g} = \left(A \oplus g\right) \Theta g \tag{3}$$

In formula, A——binary image, g——structural element, $\oplus$ —— represents the expansion of A with g expansion, Θ ——represents the closed operation of g on $\left(A \oplus g\right)$.

1）Firstly, the structural element g is used to expand the image A, such as formula (4).

$$\left(A \oplus g\right) = \left\{x \mid \left(g + x\right) \cap x \neq \varnothing\right\} \tag{4}$$

2）Then use the structural element g to corrode the expanded image, as in formula (5).

$$B \Theta g = \left\{x \mid \left(g + x\right) \subseteq A\right\} \tag{5}$$

As shown in Fig.2, the salt and pepper noise and some small area pixel interference in the binary image have been obviously eliminated, and the overall contour of the plant stems and leaves is not affected.

a. Binary image b. Images after morphological processing

Fig.2 Binary image and morphological processing image

3.Dynamic region of interest (ROI) acquisition and image segmentation

The super green feature algorithm is a technique used to extract green features by isolating the three channels of RGB images and analyzing the discrepancies in pixel values. Nevertheless, this method is susceptible to illumination variations, which may result in the neglect of certain small areas of green features. To address this issue, the extraction of green features can be enhanced by utilizing the HSV color space transformation. This method aims to binarize the green part of the image using HSV thresholding, and then perform a bitwise AND operation on the resulting mask and the original image to extract the green features. However, if the threshold range is set too wide, it may result in the extraction of similar color features as well. To fully leverage the benefits of both methods, they can be effectively combined. To begin with, the green feature pixels extracted by the two methods are horizontally projected. Subsequently, the projection data is weighted and averaged to produce smooth curve data. Finally, the least squares fitting method is utilized to further refine the data, resulting in a more accurate reflection of the green content in the image. By employing this enhanced method, it is possible to minimize the number of missing green feature pixels from the super-green feature algorithm, while also compensating for any redundant pixels extracted through HSV space transformation. This approach yields more precise green feature extraction results, offering a better representation of the green content within the image. As shown in Fig.3

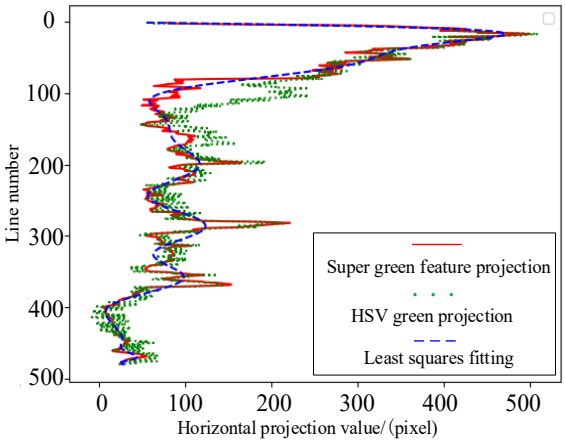

Fig.3 Horizontal projection

In the image of the cornfield captured by the camera, the corn plants that are farther away are typically smaller compared to the ones closer. Additionally, these images can have some issues, such as target adhesion, blurriness, and difficulty in distinguishing between connected domains of the plants. Therefore, relying solely on the data points of pixels has lesser reference significance for images [17]. The traditional method of acquiring a static region of interest is effective for processing specific images, but it has some issues in actual testing. These problems include the loss of important information and the inadequate processing effect of interference areas. To address these problems, this paper presents a dynamic algorithm for recognizing the region of interest. The algorithm is based on the constraint of pixel thresholds. The algorithm determines the region of interest by setting the pixel threshold and dynamically adjusts according to the characteristics of the image. This can better retain important information and reduce the impact of interference areas. By implementing this enhanced method, the region of interest in the corn field image can be identified with higher accuracy, thereby improving the effectiveness of image processing. Additionally, this algorithm is capable of adapting to the specific attributes of various images, ensuring more dependable outcomes.

Upon observing the projection image, one can determine that the range of the abscissa is 0-100 lines. Moreover, the image predominantly comprises green pixels; however, the majority of these pixels appear to be interference areas. To determine the dynamic region of interest, the abscissa that corresponds to the peak value of the fitting curve can be selected as the demarcation point to eliminate the interfering area above the image and preserve only the genuine region of interest. This not only increases the accuracy, but also reduces the computational burden. The processing time of this method is only 14 milliseconds, and the processing result is shown in Fig.4 (a). In order to get a comparison, a technique is proposed

in the Reference to derive the trapezoidal dynamic region of interest based on the vertex position. However, this method takes a long time of 20 milliseconds, and the processing results lose some important information points, and some interference areas are not eliminated, as shown in Fig.4 (b). The comparison results clearly indicate that the dynamic region of interest recognition algorithm, which is based on a pixel threshold constraint, performs exceptionally well in terms of accuracy and computational efficiency. This algorithm is capable of preserving important information while eliminating interference areas, thereby offering more reliable processing outcomes.

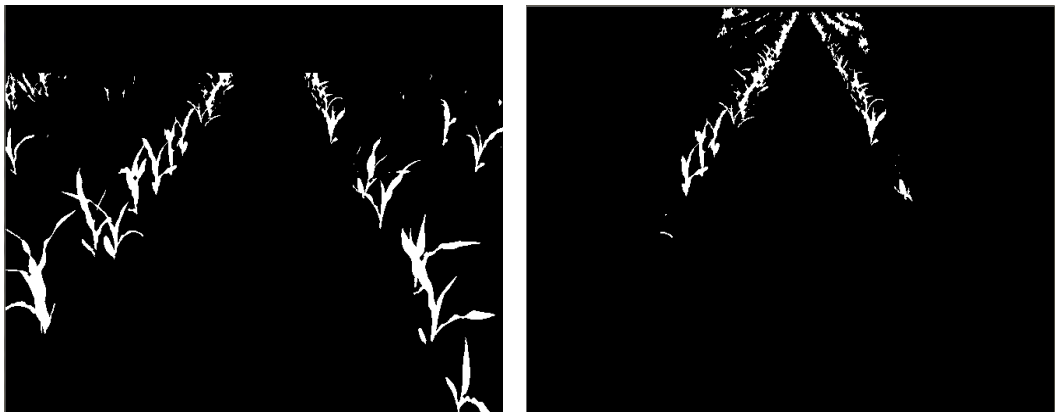

a. Proposed algorithm b. Document [18] Algorithm

Fig.4 Dynamic region of interest

To further enhance the accuracy of navigation line recognition, the image can be segmented. Initially, the white pixels on the x-axis in Figure 2 (b) are accumulated to create a vertical projection image. Then, the polynomial fitting method is used to fit the projection image, and the fitting times can be selected 10 times, 20 times and 30 times. At the same time, the fitting curve is smoothed, as shown in figure 5. After comparing, it is determined that the use of the 30-order polynomial to fit the curve results in an ordinate error between the minimum value of the fitted curve and the minimum value of the original curve that falls within the acceptable range. In order to control the processing time, the number of fittings is no longer increased. Therefore, the y-coordinate at the minimum value of the 30th-order polynomial fitting curve can be chosen as the segmentation boundary to separate the image into its left and right portions. This segmentation method can accurately determine the boundary of the region of interest, thereby enhancing the recognition accuracy even more. At the same time, the processing time is also controlled due to the control of the number of fittings.

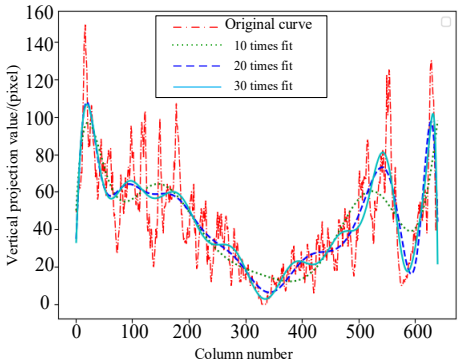

Fig.5 Vertical projection

4.Improved RANSAC and center point fitting

The RANSAC algorithm is a robust fitting algorithm that is frequently employed for extracting straight lines from images. To address the issues that traditional algorithms may face when extracting navigation lines, this paper suggests an enhanced RANSAC method. Firstly, the segmented image is displayed in the coordinate system in the form of pixels. These pixels will be divided into local points and external points. Next, the improved RANSAC algorithm is utilized to classify these pixels, determining the local points and eliminating the external points. The algorithm itself performs iterative optimization, allowing for further iterative corrections on the segmented image to more accurately determine sample clustering and improve the accuracy of the initial supervised learning sample classification. Then, the robust regression method is used to fit each cluster center to obtain the left and right navigation baseline. Finally, the navigation line is determined by finding the angular bisector of these two navigation reference lines. Through this improved method, the plant center search error caused by the adhesion of the connected domain of the green plant can be avoided, thereby reducing the deviation of the navigation line.

4.1 Focus improved RANSAC algorithm

In the experiment, the proportion of the internal point in the data is t , and the calculation method of t is as follows:

$$t=\frac{n_{inliers}}{n_{inliers}+n_{outliers}} \tag{6}$$

There are N points in the iteration process, and the probability of at least one outer point in each iteration is P_1 .The calculation method is as follows:

$$P_1=1-t^N \tag{7}$$

Iterate k times, and the probability that all k iterations have at least one outer point is P_1^k . After k iterations, the correct N local points can be sampled to calculate

the probability of the model, which is the complement of the above probability. The formula is as follows:

$$P = 1 - P_1^k = 1 - \left(1 - t^N\right)^k \tag{8}$$

Take the logarithm on both sides of the above equation, as follows:

$$k = \frac{\log\left(1 - P\right)}{\log\left(1 - t^N\right)} \tag{9}$$

The k value is set to 6. At this point, the algorithm has met the stop condition with the number of internal points, resulting in the division of internal and external points. The segmented image is then clustered and the result is shown in Fig 6. The clustering results indicate that a total of 6 clustering centers were identified on both the left and right sides of the corn rows. These clustering centers were very close to the positions of the corn rows on the pre-extracted navigation lines. Only a few abnormal points deviate from the expected position, but these deviations are within the allowable error range.

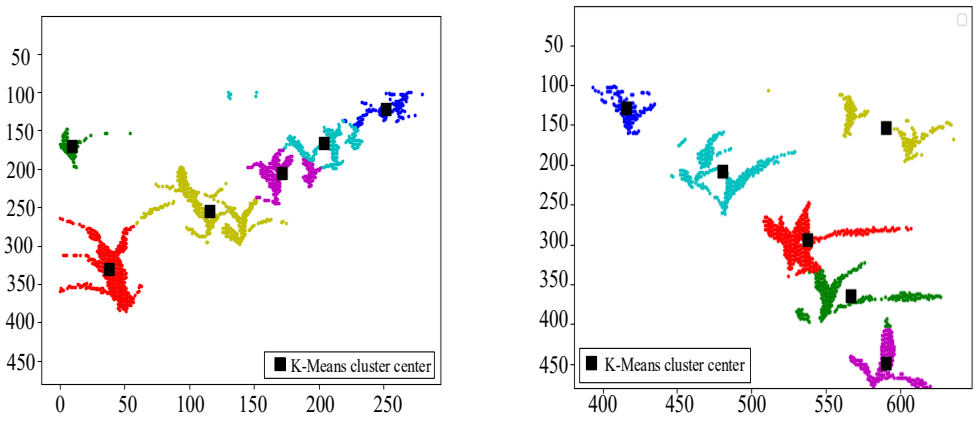

a. Left corn row clustering b. Right corn row clustering

Fig.6 Corn center clustering

4.2 Clustering center point fitting based on robust regression

The RANSAC algorithm effectively eliminates the outliers and retains the interior points. In order to ensure the accuracy of the navigation line extraction, the outliers are removed again, and the Theil-Sen estimator of the robust regression method is introduced [19-20]. Enhances the robustness of multidimensional data estimation by extending the concept of median and effectively removing outliers during clustering. The regression equation is as follows:

$$y = \alpha + \beta x + \varepsilon \tag{10}$$

In the formula, α, β —the parameters of the model

ε —Random error of the model

The Theil-sen estimation process is as follows:

$$\beta_i = \frac{y_j - y_i}{x_j - x_i} \qquad \left\{ x_i \neq x_j, i < j, i = 1,...n \right\} \tag{11}$$

In this formula, y_j and y_i are the time series values $(j > i)$ of the j and i samples, $N = \frac{n(n-1)}{2}$.

Arranging the N values β_i from smallest to largest, and the median slope is:

$$\beta_{med} = \begin{cases} \beta_{[(N+1)/2]} & N \in odd \\ \dfrac{\beta_{[N/2]} + \beta_{[(N+2)/2]}}{2} & N \in even \end{cases} \tag{12}$$

β_{med} reflects the steepness of the data trend. β_{med} greater than zero indicates that the sample has an upward trend, and vice versa.

$$\alpha = Median\left\{ y_i - \beta x_i : i = 1,..., n \right\} \tag{13}$$

The median of the slope $\frac{y_i - y_j}{x_i - x_j}$ formed by all the sample points is taken as the slope β of the fitting line, and then the linear intercept α is determined by the median of $y_i - \beta x_i$. The robust regression method is used to fit the clustering center to the left and right navigation baselines, and the angular bisector of the two is the navigation line. The slope of the robot navigation line is β, and the slopes of the left and right navigation datum lines are β_1 and β_2, according to the relationship that the tangent of the angle between β and β_1 is equal to the tangent of the angle between β and β_2, the slope β of the navigation line of the plant protection robot is calculated (as shown in Fig. 7), and its calculation formula is as follows:

$$\frac{\beta - \beta_1}{1 + \beta\beta_1} = \frac{\beta_2 - \beta}{1 + \beta\beta_2} \tag{14}$$

The final regression equation is determined by the intersection of the left and right navigation baselines as (x_0, y_0) and the slope β of the navigation baseline:

$$y - y_0 = \beta(x - x_0) \tag{15}$$

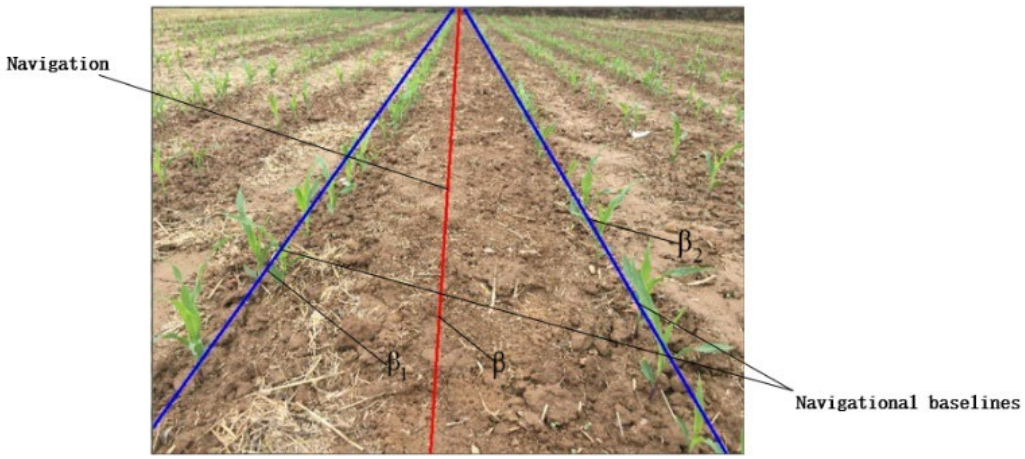

Fig.7 Corn seedling navigation line and navigation baseline

5. Experiment results and analysis

5.1 Testing material

In order to verify the real-time and accuracy of the algorithm for robot navigation line extraction, this experiment uses AGV robot, equipped with Intel Pentium(R) CPU G3250 @ 3.20GHZ, 4GB RAM, Windows 7 (64-bit) operating system computer, and programmed in Python3.7 (Anaconda) integrated development environment. The agricultural robot in the experiment is 45cm wide and 60cm long. It is equipped with monocular camera, RTK-GPS, IMU, 4G module and other sensors to collect the information of the front environment and corn plants. As shown in Fig.8.

Fig. 8 Image acquisition prototype

5.2 Navigation line extraction test and analysis

This paper uses artificial fitting as the measurement standard in order to verify the accuracy of the algorithm for extracting the center line of maize seedlings. The specific method involves manually drawing straight lines on the experimental image to represent maize seedlings, and then calculating the average value of these lines to establish a reference straight line for the seedlings. The angle between the actual extracted corn seedling center line and the artificially fitted corn seedling center line is the error angle. If the error angle is greater than 5°, the extracted corn seedling line is invalid.

To verify the reliability of the algorithm in this paper, experiments were conducted in corn seedling fields under different conditions, including fields with no seedlings, fields with weeds, fields with wheat straw, and the edge of the corn seedling field, as shown in Fig 9. The corn field at the 3-5 leaf stage was tested under four different environmental variables.

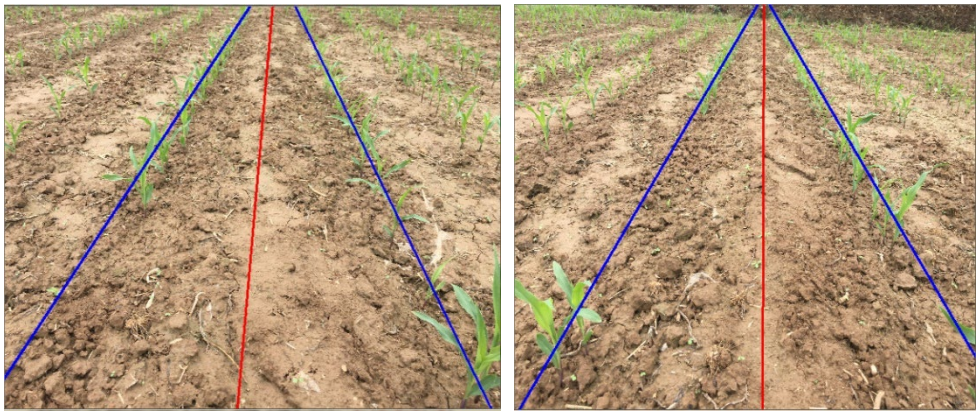

a. Lack of seedling environment

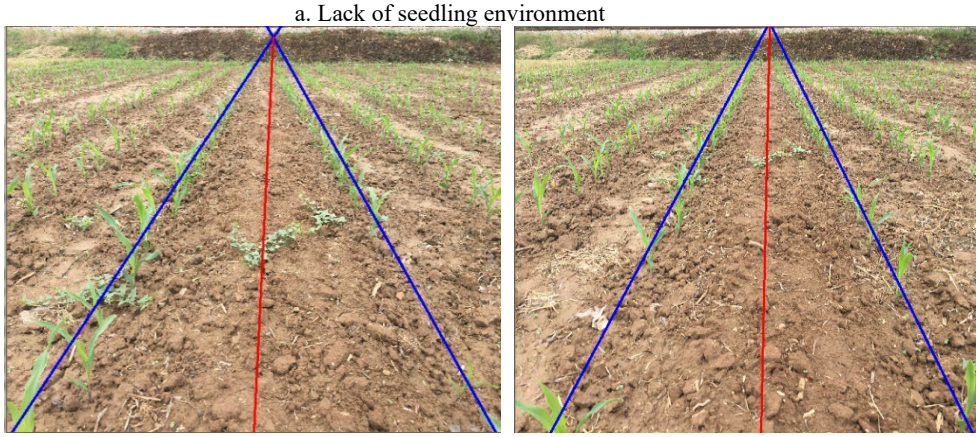

b. Weed environment

c. Wheat straw environment

d. End of the corn field

Fig.9 Navigation line extraction in different environments

The results show that the algorithm of this paper can still extract the navigation lines accurately and efficiently under the above complex situations. Since real-time and correctness are the right indexes for navigation line extraction, the average processing time as well as the accuracy of this paper's algorithm for 900 frames of images with different values of iteration number and different algorithms are statistically presented in Table 1 and Table 2:

Table 1

Performance evaluation index

K value	Average processing time	Processing frame number	Correct number of frames	Correct rate	Mean error angle
4	62.76ms	900	813	90.11%	3.197°
5	70.15ms	900	835	92.67%	2.580°
6	83.61ms	900	856	95.12%	1.671°
7	128.34ms	900	873	97%	1.139°

Table 2

Comparison of the performance of each algorithm

Arithmetic	Average processing time	Processing frame number	Correct number of frames	Correct rate	Mean error angle
Hough	62.76ms	900	713	90.11%	3.197°
SUSAN	70.15ms	900	835	92.67%	2.580°
The algorithms in this paper	83.16ms	900	856	95.12%	1.671°
Least square (estimate)	128.34ms	900	873	97%	1.139°

It can be seen from Table 1 that with the increase of value, the average processing time increases, and the correct rate also increases. By comparison, it is most reasonable when the value increases to 6, and the average processing time and error angle meet the requirements. The value continues to increase the accuracy rate, but the processing time increases greatly, which does not meet the real-time requirements, so the value is 6, As can be seen from Table 2, the average processing time and correct rate of this paper's algorithm are higher than other algorithms, which fully satisfy the indexes of real-time and correctness of navigation line extraction.

In summary, the analysis of Table 1 shows that the algorithm can adjust to different complex environ-mental conditions in the corn field to extract the navigation line of the plant protection robot, with an average image processing time of less than 85ms. The extraction accuracy of the navigation line can exceed 95%, which offers a visual navigation reference method for the automatic navigation of the plant protection robot.

6. Conclusion

（1）The improved super-greening algorithm and morphological processing are used for image preprocessing. A dynamic interest determination method based on pixel threshold constraint is proposed. This method sets the corresponding color threshold in the HSV space transformation, and extracts the green features through the mask operation, so as to make up for the defect that the hyper-greening algorithm may lose information when receiving interference.

（2）The RANSAC algorithm has been enhanced, and iterative optimization is continuously refined to extract internal points and eliminate external points in order to determine the clustering center of the corn seedling belt. The algorithm is used to process 900 random frames of images. The average processing time is only 83.61 milliseconds, and the accuracy rate is as high as 95.12%, which addresses the issue of long processing times with traditional algorithms. It has good robustness in the presence of missing seedlings, weeds, straw and other complex environments.

Acknowledgement:

This work was funded by the Key Research and Development Program of Shandong Province (Major Innovative Project in Science and Technology) (2020CXGC010804), Shandong Provincial Natural Science Foundation (ZR2021MC026).

REFERENCES

[1] *ARavind K R,Raja P,Perez-Ruiz M.* Task-based agricultural mobile robots in arable farming: a review [J]. Spanish Journal of Agricultural Research,2017,15(1):1-16.

[2] *F. Rovira-Mas,Q. Zhang,J. F. Reid,J. D.* Will.Hough-transform-based vision algorithm for crop row detection of an automated agricultural vehicle[J].Proceedings of the Institution of Mechanical Engineers, Part D. Journal of Automobile Engineering,2005,219(d8)

[3] *Kondo N.T ing K C*. Robotics for bioproduction system [M].Michigan:American Society of Agricultural Engineering Publisher.1998.

[4] *Liang Xifeng, Miao Xiangwen, Cui Shaorong, etc.* Kinematics Optimization and Simulation Test of Tomato Harvesting Manipulator [J]. Agricultural Machinery, 2005, (07):96-100.

[5] *Zhang Jian.*Supporting and leading agricultural modernization with agricultural mechanization [J].Hebei Agricultural Machinery, 2018 (02):27.

[6] *Zhang Linjie, Zhang Wenai, Han Yingzheng, et al.*Development analysis of key technologies of agricultural machinery navigation [J].Research on agricultural mechanization, 2016,38 (06):10-15 + 25.

[7] *Liao Juan, Wang Yao, Yin Junnan et al.* Centerline extraction of seedling rows based on sub-regional feature point clustering [J]. Agricultural Machinery Journal, 2019,50 (11):34-41.

[8] *Zhang Xiya,Li Xiaona,Zhang Baohua,Zhou Jun,Tian Guangzhao,Xiong Yingjun,Gu Baoxing.*Automated robust crop-row detection in maize fields based on position clustering algorithm and shortest path method[J].Computers and Electronics in Agriculture,2018,154()

[9] *Ma Hongxia, Ma Mingjian, Ma Na et al.* Agricultural machinery visual navigation baseline recognition based on Hough transform [J]. Agricultural Mechanization Research, 2013,35 (04): 37-39 + 43.

[10] *Jin Hailong, Yu Qingcang, Zhou Zhiyu, etc.* Extraction of seedling row centerline based on Meanshift and Hough transform [J]. Journal of Zhejiang University of Technology, 2015,33 (05): 405-409.

[11] *Lai Hanrong, Zhang Yawei, Zhang Bin et al.* Design and experiment of visual navigation system for corn weeding robot [J]. Transactions of the Chinese Society of Agricultural Engineering (Transactions of the CSAE), 2023,39 (01):18-27.

[12] *Gong Jinliang, Sun Ke, Zhang Yanfei, etc.* Extraction method of maize rhizome positioning navigation line based on gradient descent and corner detection [J]. Transactions of the Chinese Society of Agricultural Engineering (Transactions of the CSAE), 2022, 38 (13):177-183.

[13] *Liu Yiting, Wu Qingzheng, Lu Yuhao, etc.* Navigation line extraction method based on monocular vision for inter-row robots [J]. Chinese Journal of Inertial Technology, 2022,30 (06):777-782 + 790.

[14] *Gao Xia.* Research on road detection method in visual navigation of weeding robot-based on DSP image depth processing [J].Research on agricultural mechanization, 2020,42 (04):250-253 + 263.

[15] *Li Yong, Ding Weili.* Visual navigation line extraction algorithm for agricultural machinery based on dark channel [J].Journal of Optics, 2015,35 (02):229-236.

[16] *Zhang X Y, Li X N, Zhang B H, et al.* Automated robust crop-row detection in maize fields based on position clustering algorithm and shortest path method[J].Computers and Electronics in Agriculture, 2018, 154:165-175.

[17] *Wang Jinhua, Yan Weisheng, Liu Xulin, etc.* Research on simulation technology of lens imaging process based on visual channel [J]. Journal of System Simulation, 2010,22 (09):2131-2135.

[18] *Yang Yang, Zhang Boli, Cha Jiayi, etc.* Real-time extraction of maize inter-row navigation lines [J]. Transactions of the Chinese Society of Agricultural Engineering (Transactions of the CSAE), 2020,36 (12): 162-171.

[19] *Xueqin Wang.*Asymptotics of the Theil-Sen estimator in the simple linear regression model with a random covariate[J].Journal of nonparametric statistics,2005,17(1):p.107-120

[20] *Xueqin Wang,Qiqing Yu.* Unbiasedness of the Theil-Sen estimator[J].Journal of nonparametric statistics,2005,17(6):p.685-695